Mon. Not. R. Astron. Soc. **307**, 58–66 (1999)

The distribution of the warm and dense molecular gas around Cepheus A HW 2

J. M. Torrelles,[1,2] J. F. Gómez,[3] G. Garay,[4] L. F. Rodríguez,[5] L. F. Miranda,[2] S. Curiel[5] and P. T. P. Ho[6]

[1]*Institut d'Estudis Espacials de Catalunya (IEEC/CSIC), Edifici Nexus, C/ Gran Capità 2-4, E-08034 Barcelona, Spain*
[2]*Instituto de Astrofísica de Andalucúa, CSIC, Apdo. Correos 3004, E-18080 Granada, Spain*
[3]*Laboratorio de Astrofísica Espacial y Física Fundamental, INTA, Apdo. Correos 50727, E-28080 Madrid, Spain*
[4]*Departamento de Astronomía, Universidad de Chile, Casilla 36-D, Santiago, Chile*
[5]*Instituto de Astronomía, Universidad Nacional Autónoma de México, Apdo. Postal 70-264, DF 04510, México*
[6]*Harvard–Smithsonian Center for Astrophysics, 60 Garden Street, Cambridge, MA 02138, USA*

Accepted 1999 February 22. Received 1999 February 19; in original form 1999 January 25

ABSTRACT

We present VLA observations of the $(J, K) = (1, 1)$, (2, 2), (3, 3) and (4, 4) inversion transitions of NH_3 toward the HW 2 object in Cepheus A, with 1-arcsec angular resolution. Emission is detected in the main hyperfine line of the first three transitions. The NH_3(2, 2) emission shows a non-uniform 'ring' structure, which is more extended (3 arcsec) and intense than the emission seen in the (1, 1) and (3, 3) lines. A rotational temperature of ~ 30–50 K and a lower limit to the mass of $\sim 1\ (X_{NH_3}/10^{-8})^{-1}\,M_\odot$ are derived for the ring structure. The spatio-kinematical distribution of the NH_3 emission does not seem to be consistent with a simple circumstellar disc around the HW 2 thermal biconical radio jet. We suggest that it represents the remnant of the parental core from which both the inner 300-au (0.4 arcsec) disc, traced by the water maser spots previously found in the region, and the central object have formed. The complex velocity field of this core is probably produced from bound motions (similar to those of the inner disc) and from interaction with outflowing material.

Key words: stars: pre-main-sequence – ISM: individual: Cepheus A – ISM: jets and outflows – ISM: molecules – radio lines: ISM.

1 INTRODUCTION

The search for circumstellar discs around young stellar objects (YSOs) is one of the major subjects of current star formation studies. There is now considerable evidence that such discs (protoplanetary discs) are present around low-mass young stars (e.g. Shu, Adams & Lizano 1987; Lizano & Torrelles 1995; Rodríguez et al. 1998; Torrelles et al. 1998). However, there is very little evidence that these discs are also present around high-mass young stars (Plambeck, Wright & Carlstrom 1990; Nakamura et al. 1991; Lada & Adams 1992; Planesas, Martín-Pintado & Serabyn 1992).

The HW 2 (Hughes & Wouterloot 1984) thermal biconical radio jet (Rodríguez et al. 1994), located in the high-mass star formation region Cepheus A East (Sargent 1977; at 725-pc distance: Johnson 1957), is one of the few known objects associated with a massive YSO (e.g., Cohen, Rowland & Blair 1984; Garay et al. 1996) where the presence of a circumstellar disc has been inferred (Torrelles et al. 1996, hereafter T96). Water maser observations show a band of maser spots with their spatial and velocity distribution tracing a disc of ~ 300-au radius (~ 0.4 arcsec) (hereafter the 'water maser disc'). This disc, simultaneously undergoing rotation and contraction, is oriented perpendicular to the biconical radio jet and probably constitutes the smallest circumstellar disc observed around a massive YSO (T96). Observations of the NH_3(1, 1) line with ~ 2.3-arcsec angular resolution show the presence of a dense molecular core, centred on the HW 2 object, with a deconvolved size of 3.3×2.3 arcsec^2 ($\simeq 2400 \times 1700$ au: Torrelles et al. 1993a, hereafter T93). Although this NH_3 dense core was originally interpreted as a circumstellar molecular disc (T93), its orientation at PA $\simeq$ 30°–40° precludes a clear relationship with the water maser disc of 300-au radius, which is oriented at PA $\simeq -48°$ (T96). On the other hand, the SiO molecule (Gómez et al. 1999) traces a structure that is consistent with an outer (750-au radius) disc with a similar orientation to the water maser disc.

In this paper we report NH_3(1, 1), (2, 2), (3, 3) and (4, 4) line observations toward HW 2, carried out with the Very Large Array

© 1999 RAS

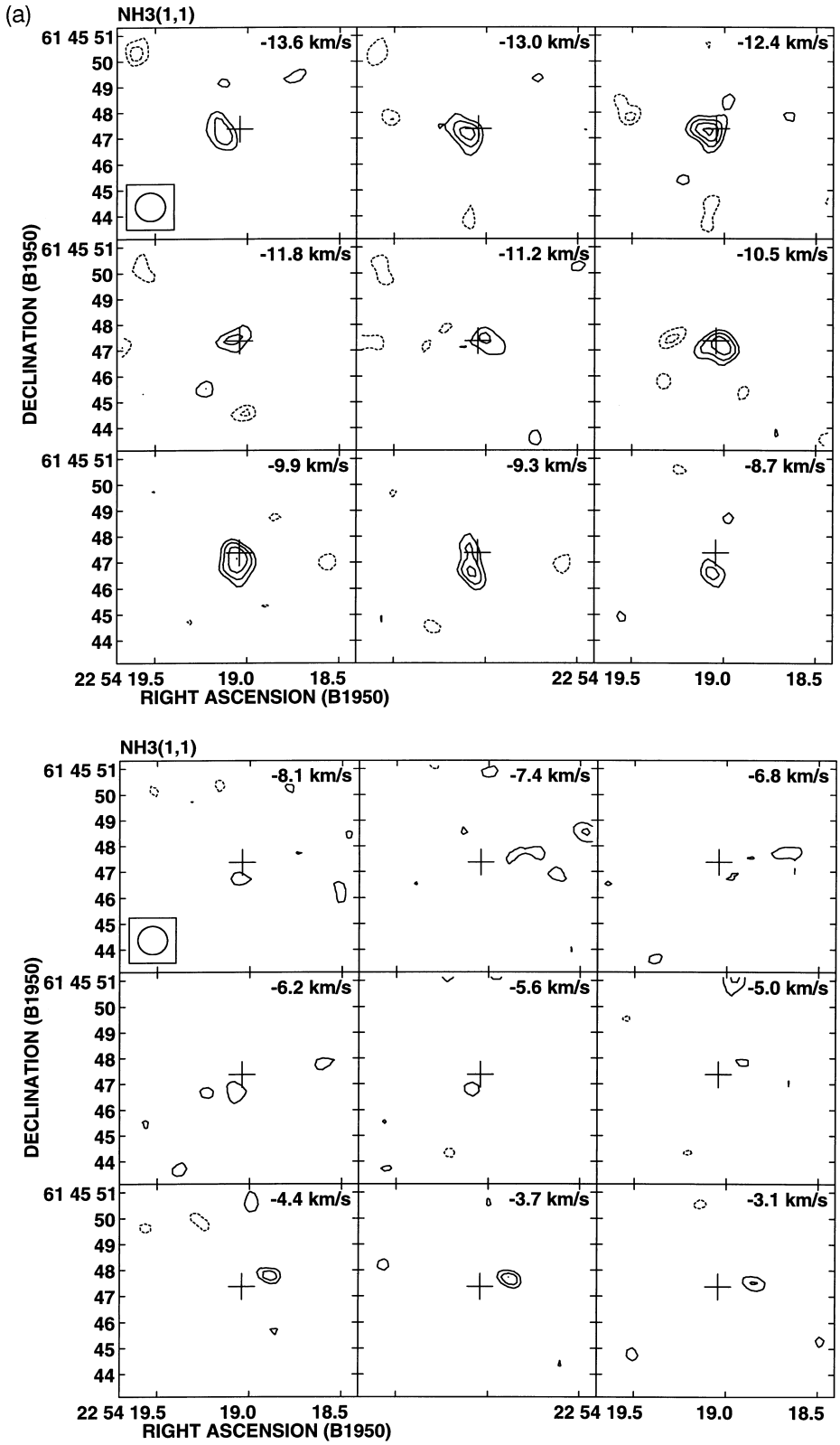

Figure 1. Channel maps of the $NH_3(1, 1; m)$ (a), $NH_3(2 , 2; m)$ (b) and $NH_3(3, 3; m)$ (c) emission. V_{LSR} is indicated in each panel. For the (3, 3) transition the velocity channels in the -8.1 to $-3.1\,km\,s^{-1}$ range are not shown here, since emission was not detected in this range. Contour levels are -4, -3, 3, 4, 5, 6, 7 and $8 \times 2.6\,mJy\,beam^{-1}$, the rms noise level of the maps. The half-power contour of the synthesized beam ($1.15 \times 1.09\,arcsec^2$, PA 90°) is indicated in the lower left-hand corner of the first panel for each ammonia transition. The cross indicates the position of the HW 2 biconical radio jet.

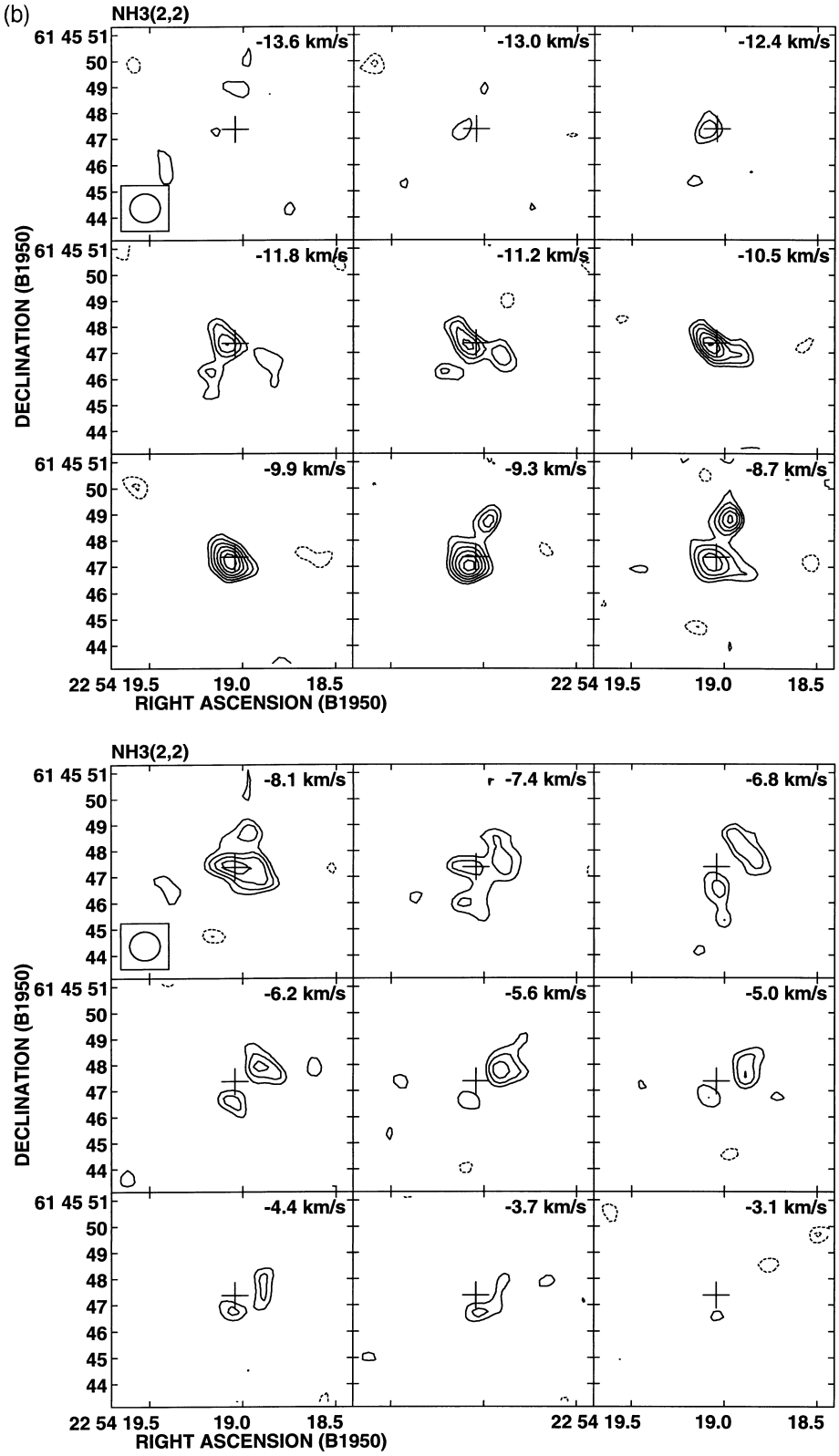

Figure 1 – *continued*

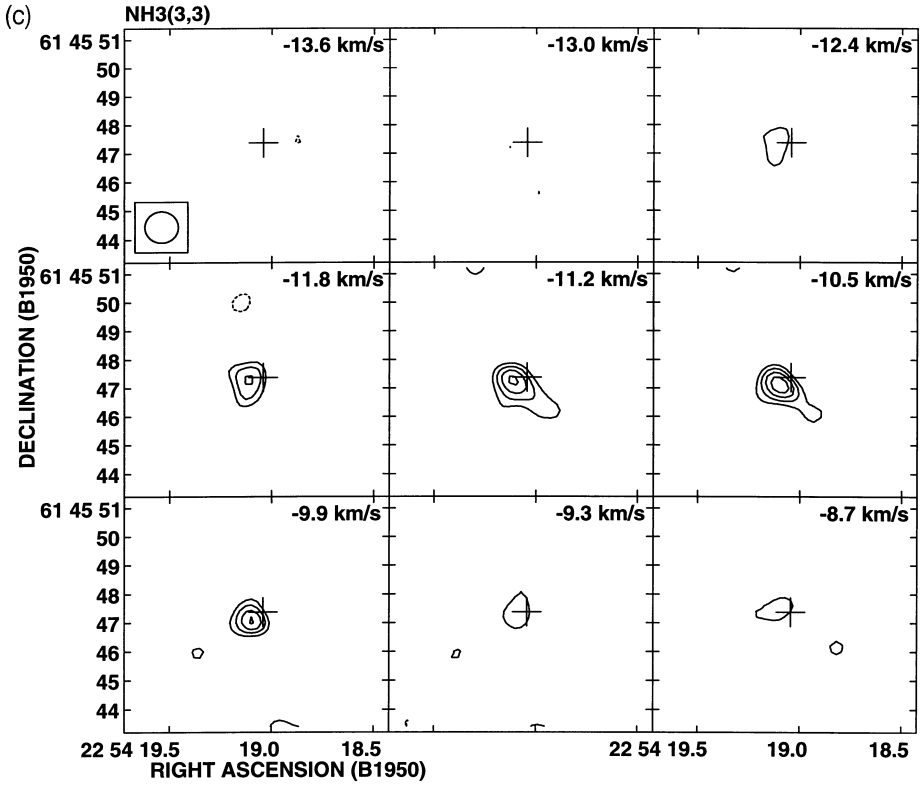

Figure 1 – *continued*

(VLA) in its C-configuration, which provides an angular resolution of $\simeq 1$ arcsec ($\simeq 700$ au at the Cepheus A distance), which have been obtained with higher sensitivity and angular resolution than the previous ammonia observations. Our main goal with these observations was to gain insights into the kinematics and temperature distributions of the high-density molecular gas around HW 2 in order to clarify its relationship with the water maser disc. The observations of the four inversion lines of ammonia were selected to sample a wider range in the physical conditions of the ammonia gas around HW 2. In fact, given the high temperatures found in this core ($T_{\rm K} \gtrsim 50$ K with a beam of $\simeq 5$ arcsec: Torrelles et al. 1993b), an important fraction of the molecular gas could be 'hidden' for the lower excitation ammonia lines.

2 OBSERVATIONS

The observations were made with the VLA of the National Radio Astronomy Observatory (NRAO)[1] in its C-configuration, in two runs of 10 h each, during 1993 August 10 [NH_3(1, 1) and NH_3(2, 2) transitions; $\nu_{11} = 23\,694.4955$ MHz, $\nu_{22} = 23\,722.6336$ MHz] and 1996 March 18 [NH_3(3, 3) and NH_3(4, 4) transitions; $\nu_{33} = 23\,870.1296$ MHz, $\nu_{44} = 24\,139.4169$ MHz]. We used the 4IF spectral line mode to observe in each run two different rotational ammonia transitions simultaneously. Each line was observed in right and left circular polarization with a bandwidth of 3.125 MHz split into 64 channels of 48.828-kHz spectral resolution ($\simeq 0.6\,{\rm km\,s^{-1}}$ at $\lambda = 1.3$ cm). The central channel local standard of rest (LSR) velocity of the bandwidth for each line was set to $-11.15\,{\rm km\,s^{-1}}$, covering a velocity range $-30 \lesssim {\rm V_{LSR}} \lesssim 8\,{\rm km\,s^{-1}}$. This velocity range encompasses in the (1, 1) and (2, 2) ammonia observations the main [(1, 1; m), (2, 2; m)] and inner [(1, 1; is), (2, 2; is)] satellite hyperfine components, while in the (3, 3) and (4, 4) observations it covers only the main hyperfine component [(3, 3; m), (4, 4; m)] (see Ho & Townes 1983). Calibration and further image processing were performed using standard procedures of the Astronomical Image Processing System (AIPS) software of NRAO. The continuum emission contribution from the HW 2 source to the spectral line data was subtracted from all the individual channels using the task UVLIN of AIPS (see Cornwell, Uson & Haddad 1992).

Cleaned maps of the individual channels were obtained with natural weighting of the (u, v) data, providing a synthesized beam of $\simeq 1$ arcsec. Hanning smoothing to the velocity axis of the data was applied, giving a final velocity resolution of $\simeq 1.2\,{\rm km\,s^{-1}}$. The achieved rms noise level of the individual channels of the four ammonia lines (after Hanning smoothing) was $\simeq 2.6\,{\rm mJy\,beam^{-1}}$, a factor of 2 better than that achieved in the previous ammonia observations by T93. With these particular angular and velocity resolutions we detected emission in the main hyperfine component of the (1, 1), (2, 2) and (3, 3) ammonia transitions toward HW 2 (Fig. 1). No emission was detected in the NH_3 (4, 4) line at a 4σ level of $\simeq 10\,{\rm mJy\,beam^{-1}}$ (maps are not shown here). This implies a lack of detectable amounts of gas with rotational temperatures $\gtrsim 50$ K (see also below). The satellite hyperfine components of the (1, 1) and (2, 2) transitions were also not detected at this 4σ level. No ammonia emission was detected toward the other HW radio continuum sources observed in the Cepheus A East region (Hughes & Wouterloot 1984; Hughes, Cohen & Garrington 1995) with this particular angular and velocity resolution [see Garay

[1] The NRAO is a facility of the National Science Foundation operated under cooperative agreement by Associated Universities, Inc.

et al. (1996) for a discussion on the nature of the radio objects in the Cepheus A East region].

3 RESULTS AND DISCUSSION

3.1 Spatial distribution of the (1, 1), (2, 2) and (3, 3) ammonia emission

Fig. 1 shows the individual channel contour maps of the (1, 1; m) (a), (2, 2; m) (b) and (3, 3; m) (c) line emission, made with the same synthesized beam (1.15×1.09 arcsec^2, PA90°) (*uv* coverage was similar for all the ammonia lines). Emission in the (1, 1; m) and (3, 3; m) transitions is detected roughly over the same velocity range ($-13 \lesssim V_{\rm LSR} \lesssim -9$ km s^{-1}), showing similar intensities (Figs 1a and c). On the other hand, the NH_3(2, 2; m) line emission is, on average, a factor of ~ 1.5 more intense than the (1, 1; m) and (3, 3; m) emissions, is detected over a broader velocity range ($-13 \lesssim V_{\rm LSR} \lesssim -4$ km s^{-1}), and shows a more extended and complex spatial structure (Fig. 1b).

Velocity-integrated intensity maps of the emission in the main hyperfine component of the three transitions are presented in Figs 2(a)–(c). The integrated intensity map of the (2, 2; m) line extends over a region of $\simeq 3$ arcsec diameter around HW 2 (Fig. 2b), while the integrated (1, 1; m) and (3, 3; m) line emissions show a more compact ($\simeq 1.5$ arcsec diameter) structure (Figs 2a and c). This is probably due to excitation effects of the ammonia lines (see Section 3.2).

The morphology of the molecular core observed in the (1, 1; m) line around HW 2 (Fig. 2a) is consistent with that reported previously by T93 in the same line, but with lower angular resolution. The morphology of the (2, 2) emission (Fig. 2b) can roughly be described as a non-circular, non-uniform 'ring'

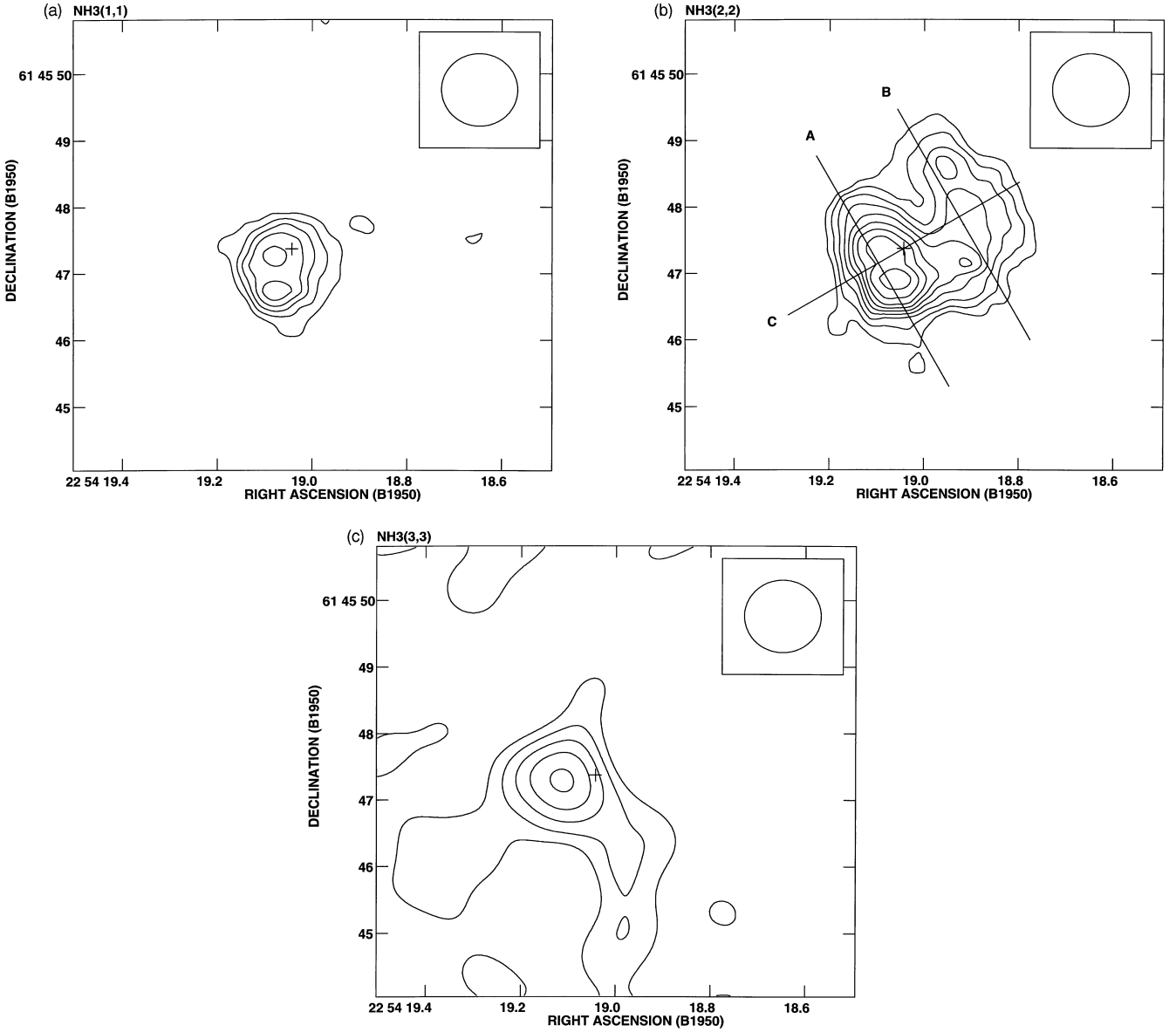

Figure 2. Contour maps of the integrated intensity of the (1, 1; m) (a), (2, 2; m) (b) and (3, 3; m) (c) ammonia lines. Contour levels are at 1, 2, 3, 4, 5, 6, 7, 8 and 9×11.4 mJy beam^{-1} km s^{-1}. Lines labelled A, B and C on (b) indicate the axes along which the position–velocity contour maps shown in Figs 4(a), (b) and (c), respectively, have been made.

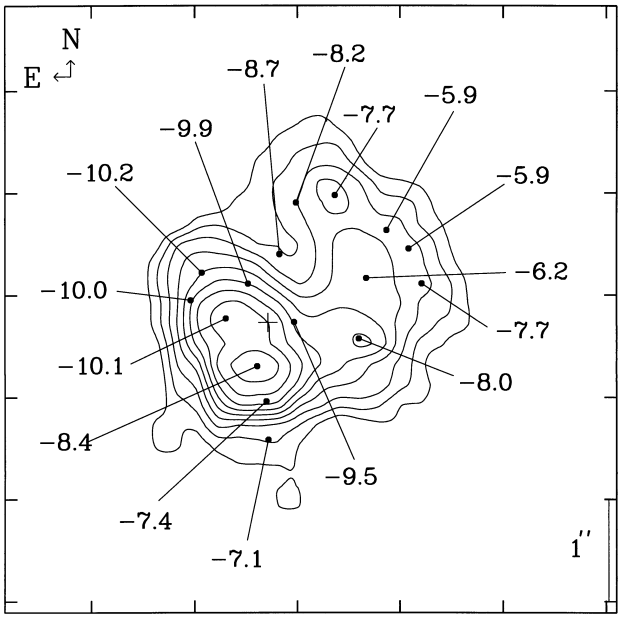

Figure 3. Velocity values (V_{LSR}/km s^{-1}) measured at selected positions through the first-order moment of the (2, 2; m) ammonia transition, superposed on the contour map of the integrated intensity of the (2, 2; m) line (Fig. 2b).

structure of ~ 3-arcsec diameter. The locations of the (1, 1; m) and (3, 3; m) emission (Figs 2a and c) coincide with the more intense south-eastern half of the (2, 2) ammonia 'ring' structure, which is closer to HW 2 than is the north-western, weaker half.

The north-western region of the (2, 2; m) structure was not detected previously by T93, who only detected the south-eastern part of the ammonia 'ring'. This was probably due to a combination of both lower angular resolution and lower sensitivity of their data ($\simeq 6$ mJy beam^{-1} per 1.2 km s^{-1}). Note that the emission from the components in the individual velocity channels (Fig. 1b) contributing to the north-western half of the (2, 2) ammonia 'ring' is at a maximum level of $\simeq 15$ mJy beam^{-1}.

3.2 Physical parameters

From the (2, 2; m) to (1, 1; m) velocity integrated line intensity ratio, an estimate of the rotational temperature describing the population of the (2, 2) and (1, 1) ammonia rotational states, $T_R(22–11)$, can be obtained ($T_R \leq T_K$, with T_K the kinetic temperature: see Ho & Townes 1983). For the region where both (1, 1) and (2, 2) emission is detected, we find a mean value of ~1.5 for the (2, 2; m)/(1, 1; m) ratio, which, assuming optically thin emission, implies a mean rotational temperature $T_R(22–11) \simeq 50$ K. On the other hand, for the weaker north-western half of the (2, 2) ammonia 'ring', where the (1, 1; m) emission was not detected, adopting for this line an upper limit value (4σ) of $\simeq 10$ mJy beam^{-1}, we obtain a lower limit of $\simeq 1.3$ for the (2, 2; m)/(1, 1; m) ratio, which implies a rotational temperature $T_R(22–11) \gtrsim 40$ K. This result suggests that probably the bulk of the structure detected in the (2, 2) ammonia line has a similar temperature. The small size of the region where the (1, 1; m) emission is detected ($\simeq 1.5$ arcsec diameter), as compared with the synthesized beam ($\simeq 1$ arcsec diameter), precludes a realistic map of the (2, 2; m)/(1, 1; m) ratio and a study of the possible temperature gradients around HW 2. Finally, from the ratio of the (3, 3; m) and (2, 2; m) components ($\simeq 0.5$), a rotational temperature $T_R(33–22) \simeq 30$ K is derived. It is also important to note that opacity effects could affect these estimates of the rotational temperatures (see Ho & Townes 1983).

From the integrated flux density of the (2, 2; m) line over a region of 3-arcsec diameter around HW 2 ($\simeq 400$ mJy km s^{-1}), assuming optically thin emission, a single rotational temperature describing the population of all the rotational levels of the ammonia molecule, $T_R = T_{ex} = 50$ K, and an abundance ratio $NH_3/H_2 = 10^{-8}$ (Herbst & Klemperer 1973), we estimate an average column density $N(H_2) \simeq 5 \times 10^{23}(X_{NH_3}/10^{-8})^{-1}$ cm^{-2}, a volume density $n(H_2) \simeq 2 \times 10^7(X_{NH_3}/10^{-8})^{-1}$cm^{-3}, and a mass $M(H_2) \simeq 1(X_{NH_3}/10^{-8})^{-1}$ M$_\odot$ within this region. This is a lower limit to the mass, given the assumption of optically thin emission. In particular, if an opacity $\tau(1, 1; m) = 1$ were adopted [such as that derived by Torrelles et al. (1993b) for the extended ammonia emission in the region], the estimated mass value would increase by a factor of ~ 1.6 [$\tau(1, 1; m)/(1-e^{-\tau(1,1;m)})$].

3.3 Kinematics of the ammonia emission

In order to study the kinematics of the high-density molecular gas around HW 2, we have produced first-order moments of the three ammonia lines. From the (1, 1; m) moment (not shown here) we find that there are velocity differences of $\simeq 4$ km s^{-1} from north to south of the core, with blueshifted velocities ($V_{LSR} \simeq -13$ km s^{-1}) toward the north and north-eastern regions, and redshifted velocities ($V_{LSR} \simeq -9$ km s^{-1}) toward the southern ones. These velocity shifts are consistent with those found by T93 in the (1, 1; m) transition.

On the other hand, the first-order moment of the (2, 2; m) line presents a rather complex velocity field, as shown in Fig. 3. The more intense south-eastern half of the (2, 2) ammonia 'ring' presents a similar velocity field to that seen in the (1, 1; m) line. Across the north-western, weaker half of the 'ring', velocity variations of $\simeq 2$ km s^{-1} are also found, with blueshifted motions to the north ($V_{LSR} \simeq -8$ km s^{-1}) with respect to those to the south ($V_{LSR} \simeq -6$ km s^{-1}).

The velocity shifts of the ammonia gas can be best appreciated in the position-velocity (PV) maps with PA 30°, along the south-eastern (Fig. 4a) and north-western (Fig. 4b) regions of the 'ring' structure. The axes selected to produce these PV contour maps are indicated in Fig. 2(b). Along the more intense half of the ring, from north-east to south-west, velocity differences of ~ 8 km s^{-1} are detected in the emission above the 4σ level (see Fig. 4a). Along the less intense half of the 'ring', velocity differences of ~ 5 km s^{-1} are observed in the emission above the same intensity level of 4σ (see Fig. 4b).

We have also made a PV contour map along a PA − 60° axis, perpendicular to the previous ones, but through the position of the HW 2 source (Fig. 4c). From this particular PV diagram we see that the two observed maxima are shifted in velocity by $\simeq 4$–5 km s^{-1}, with the north-western maximum redshifted with respect to the south-eastern one. Weaker emission above the $\simeq 4\sigma$ level shows velocity differences up to $\simeq 8$ km s^{-1} over a distance of $\simeq 3$ arcsec.

The spatio-kinematical distribution of the high-density circumstellar gas traced by the NH_3 lines, especially that observed through the (2, 2) transition, does not appear to be amenable to

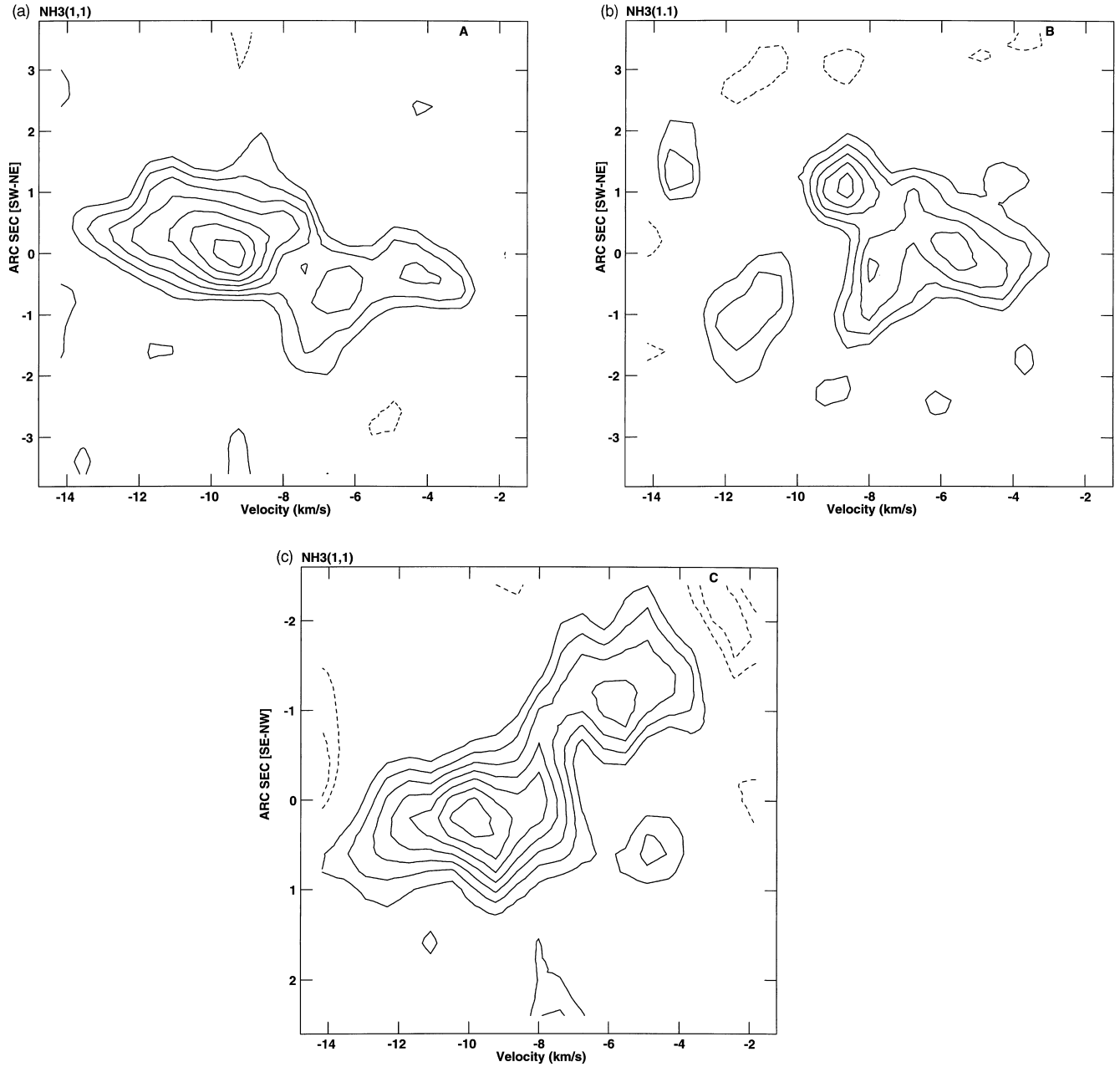

Figure 4. Position–velocity contour maps of the (2, 2; m) line along the axes A (a) (south-west to north-east), B (b) (south-west to north-east) and C (c) (south-east to north-west) indicated in Fig. 2(b). Position offsets (arcsec) are relative to $[\alpha(1950), \delta(1950)] = (22^{\rm h}\,54^{\rm m}\,19\overset{\rm s}{.}09, 61^\circ\,45'\,47\overset{''}{.}03)$ (a), $(22^{\rm h}\,54^{\rm m}\,18\overset{\rm s}{.}92, 61^\circ\,45'\,47\overset{''}{.}73)$ (b) and $(22^{\rm h}\,54^{\rm m}\,19\overset{\rm s}{.}04, 61^\circ\,45'\,47\overset{''}{.}37)$ (c). Contour levels are at -3, -2, 2, 3, 4, 5, 6, 7 and $8 \times 2.6\,{\rm mJy\,beam^{-1}}$.

interpretation in terms of a circumstellar molecular disc around HW 2, as was suggested by T93. In fact, the bipolar outflow associated with HW 2, as traced by the biconical radio jet (Rodríguez et al. 1994; T96) and the bipolar molecular HCO^+ outflow (Gómez et al. 1999), is oriented at PA $\simeq$ 45–60°. None of the structures detected in ammonia presents an orientation clearly perpendicular to the outflow, as expected for a disc/jet–outflow association.

We suggest that the core detected in ammonia around HW 2 is the remnant of the parent molecular gas from which both the inner circumstellar rotating and contracting water maser disc of 300-au radius (0.4 arcsec) (T96) and the inner central object have formed. The extended ($\simeq$ 3-arcsec) remnant structure of high-density molecular gas could share bound motions with the inner water maser disc (rotation and/or contraction), around the central object. In fact, the velocity variations observed in the ammonia gas, up to $\sim$8 km s^{-1} over distances of $\sim$ 3 arcsec (3×10^{16} cm), can indeed be bound by a central mass of 20 $M_\odot$, which could be provided by the central massive YSO related to HW 2 (e.g. Cohen, Rowland & Blair 1984; Garay et al. 1996). Furthermore, it is worth noting that the velocity differences found in the ammonia gas along the PA $-$ 60° axis through HW 2 (Fig. 4c) have the same sign as the velocity gradient observed along the band of the H_2O masers tracing the inner circumstellar disc perpendicular to the radio jet.

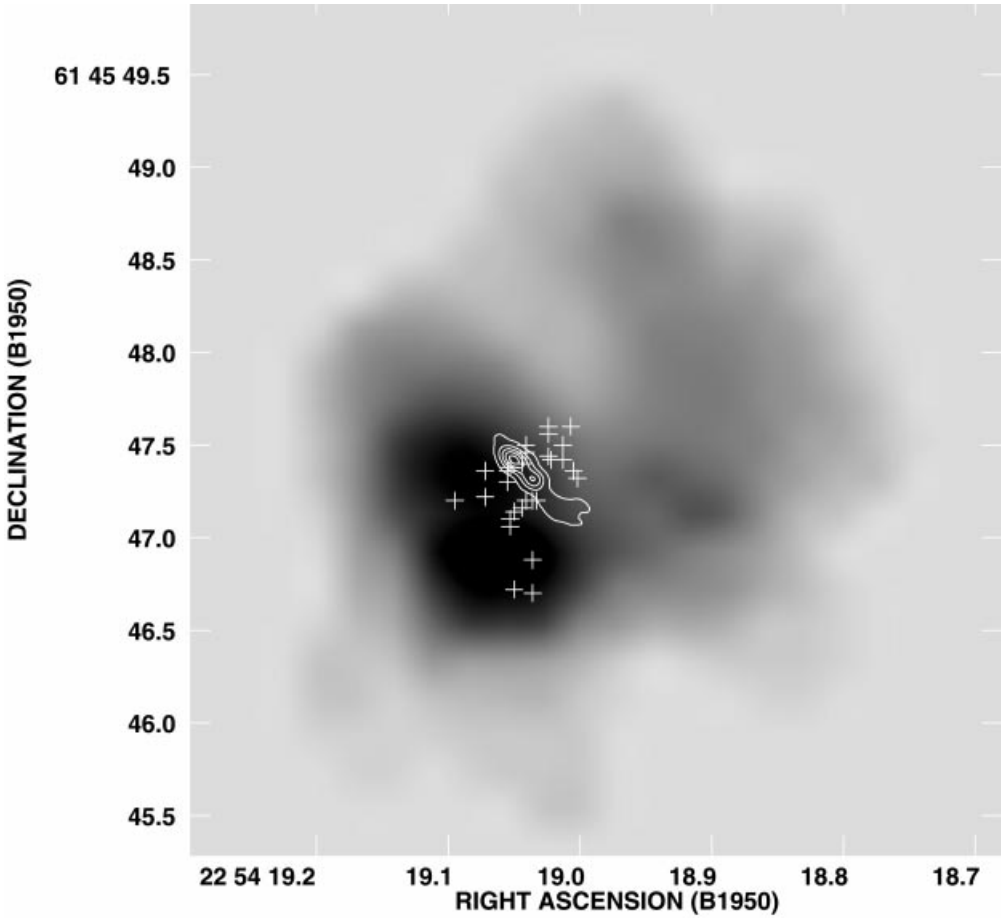

Figure 5. A contour map of the HW 2 thermal radio jet in 1.3-cm continuum, and positions of the H_2O maser spots (crosses) detected in the region (from T96), superposed on the integrated intensity of the (2, 2; m) line (Fig. 2b of this paper; grey-scale).

We cannot discard, however, the possibility that the observed motions in the ammonia gas could have been affected by the strong outflow of the central object, disturbing both the morphology and kinematics of the original core. In Fig. 5 we show a superposition of the biconical radio jet, the water maser disc and the integrated intensity map of the (2, 2; m) emission. This figure suggests a 'cavity-like' configuration seen in the (2, 2; m) ammonia emission, flaring out on both sides away from the plane of the water maser disc. The overall blueshifted motions observed in the north-eastern regions of the (2, 2) ammonia structure, with respect to the south-western regions, has the same sense as the outflow observed in HCO^+ (Gómez et al. 1999). Hence the lower intensity ammonia emission away from the central maser disc could be material associated with the outflow.

Finally, it is interesting that, while the ammonia structure with a radius of ~ 1000 au lacks a clear rotational signature, the smaller size structures traced by the water masers (with radius of 300 au) and the SiO (with radius of 750 au: Gómez et al. 1999) do show kinematics consistent with rotation. One could expect that rotational motions will dominate over turbulent motions inside a certain radius, of order $r \simeq GM/a^2$, where G is the gravitational constant, M is the mass interior to r, and a is the turbulent velocity dispersion of the gas. Assuming $M = 20\,M_\odot$ and $a = 4\,\mathrm{km\,s^{-1}}$, we obtain $r = 1000$ au. This rough estimate suggests that only inside a radius of ~ 1000 au will we be able to start finding clear evidence of rotation, in agreement with the observations.

4 CONCLUSIONS

We have made observations of the NH_3(1, 1), (2, 2), (3, 3) and (4, 4) lines toward the HW 2 object in Cepheus A, using the VLA in its C-configuration (1-arcsec angular resolution). Our main conclusions are as follows.

(i) We have detected compact emission of the main hyperfine component of the NH_3(1, 1), (2, 2) and (3, 3) lines.

(ii) The NH_3(2, 2) emission is more extended (3 arcsec) and intense than the emission seen in the (1, 1) and (3, 3) lines, and shows a non-uniform 'ring' structure. The observed line ratios provide a strong constraint on the excitation of the gas.

(iii) A rotational temperature of ~ 30–50 K and a lower limit to the mass of $\sim 1(X_{\mathrm{NH_3}}/10^{-8})^{-1}\ M_\odot$ are derived for the ring structure.

(iv) The spatio-kinematical distribution of the NH_3 emission does not seem to be consistent with a simple circumstellar disc. We suggest that it represents the remnant core from which both the inner 300-au (0.4 arcsec) disc and the central object have formed. The complex velocity field of this remnant core could

have contributions from bound motions (similar to those of the inner disc), and from interaction with outflow material.

ACKNOWLEDGMENTS

We thank an anonymous referee for useful and valuable comments. GG acknowledges support from a Chilean Presidential Science Fellowship and from Fondecyt project 1980660. JFG, LFM and JMT are supported in part by DGICYT grant PB95-0066 and by Junta de Andalucía (Spain). JFG is also supported by INTA grant IGE 4900506. LFR and SC acknowledge the support of DGAPA, UNAM and CONACyT (México). This work has been partially supported by the Programa de Cooperación Científica con Iberoamérica. The National Radio Astronomy Observatory is a facility of the National Science Foundation, operated under cooperative agreement by Associated Universities, Inc.

REFERENCES

Cohen R. J., Rowland P. R., Blair M. M., 1984, MNRAS, 210, 425
Cornwell T. J., Uson J., Haddad N., 1992, A&A, 258, 583
Garay G., Ramírez S., Rodríguez L. F., Curiel S., Torrelles J. M., 1996, ApJ, 459, 193
Gómez J. F., Sargent A. I., Torrelles J. M., Ho P. T. P., Rodríguez L. F., Cantó J., Garay G., 1999, ApJ, 514, 287
Herbst E., Klemperer W., 1973, ApJ, 185, 505
Ho P. T. P., Townes C. H., 1983, ARA&A, 21, 239
Hughes V. A., Wouterloot J. G. A., 1984, ApJ, 276, 204
Hughes V. A., Cohen R. J., Garrington S., 1995, MNRAS, 272, 469
Johnson H. L., 1957, ApJ, 126, 121
Lada C. J., Adams F. C., 1992, ApJ, 393, L728
Lizano S., Torrelles J. M., eds, 1995, Rev. Mex. Astron. Astrofis. Ser. Conf. 1, Circumstellar Disks, Outflows and Star Formation
Nakamura A., Kawabe R., Kitamura Y., Ishiguro M., Murata Y., Ohashi N., 1991, ApJ, 383, L81
Plambeck R. L., Wright M. C. H., Carlstrom J. E., 1990, ApJ, 348, L65
Planesas P., Martín-Pintado J., Serabyn E., 1992, ApJ, 386, L23
Rodríguez L. F., Garay G., Curiel S., Ramírez S., Torrelles J. M., Gómez Y., Velázquez A., 1994, ApJ, 430, 713
Rodríguez L. F., 1998, et al., Nat, 395, 355
Sargent A. I., 1977, ApJ, 218, 736
Shu F. H., Adams F. C., Lizano S., 1987, ARA&A, 25, 23
Torrelles J. M., Rodríguez L. F., Cantó J., Ho P. T. P., 1993a, ApJ, 404, L75 (T93)
Torrelles J. M., Verdes-Montenegro L., Ho P. T. P., Rodríguez L. F., Cantó J., 1993b, ApJ, 410, 202
Torrelles J. M., Gómez J. F., Rodríguez L. F., Curiel S., Ho P. T. P., Garay G., 1996, ApJ, 457, L107 (T96)
Torrelles J. M., Gómez J. F., Rodríguez L. F., Curiel S., Anglada G., Ho P. T. P., 1998, ApJ, 505, 756

This paper has been typeset from a TEX/LATEX file prepared by the author.